Multiple Scattering of a π^- beam in the HERA-B detector.

Antonios Garas
Aristotle University of Thessaloniki
Department of Physics
Thessaloniki, Greece.
Email: agara@skiathos.physics.auth.gr

We study the effect of multiple scattering to a simulated 1 GeV beam of π^- using GEANT. The results are compared with the theoretical prediction according to Molière theory of multiple scattering.

1 Introduction

When a charged particle traversing ordinary matter, it is deflected by many small-angle scatters. Most of this deviation is due to Coulomb scattering from nuclei, and also to a lesser degree to the electron field, hence the effect is called multiple Coulomb scattering.

At least four different theories of the multiple scattering of electrons by atoms have been published by Molière [1][2], Snyder and Scott [3][4], Goudsmit and Saunderson [5], and Lewis [6], which are mathematically closely related, and which can give exact results if carefully evaluated. The first two use immediately the approximation of small scattering angles and therefore an expansion in Bessel functions. Goudsmit and Saunderson developed a theory valid for any angle by means of an expansion in Legendre polynomials. Lewis starts from the Legendre expansion and then goes over to the limit of small angles, thus establishing the connection between the first three methods.

In Molière theory, the Coulomb scattering distribution is roughly Gaussian for small deviation angles, but at larger angles (greater than a few θ_0, defined below) it behaves like Rutherford scattering, having larger tails than does a Gaussian distribution.

If we define the *spatial angle*, θ_{space}, as the difference between the angle in which the particle enters and exits the material, and the projection of this angle to a plane as θ_{plane}, then we can also define θ_0 as the r.m.s. of the angle between the directions projected on a plane of a particle before and after traversing a thickness x of a volume. θ_0 is related to θ_{space}^{rms} according to the equation:

$$\theta_0 = \theta_{plane}^{rms} = \frac{1}{\sqrt{2}}\,\theta_{space}^{rms}. \qquad (1)$$

It is sufficient for many applications to use a Gaussian approximation for the central 98% of the projected angular distribution, with a width given by [7][8]

$$\theta_0 = \frac{13.6MeV}{\beta cp} z\sqrt{x/X_0}\left[1 + 0.038ln\left(x/X_0\right)\right]. \qquad (2)$$

Here p, β c, and z are the momentum, velocity and charge number of the incident particle, and x/X_0 is the thickness of the scattering medium in radiation lengths[1]. This value of θ_0 is from a fit to Molière distribution [1][2] for single charged particles with $\beta = 1$ for all Z, and is accurate to 11% or better for $10^{-3} < x/X_0 < 100$.

Lynch and Dahl have extended this phenomenological approach, fitting Gaussian distributions to a variable fraction of the Molière distribution for arbitary scatterers [8], and achieve accuracies of 2% or better.

In our analysis we used a simulated beam of 1 GeV π^- traversing the volume of HERA-B detector using GEANT [9] Monte Carlo program. Our goal was to study the limits where formula

[1] In dealing with charged particles at high energies, it is convenient to measure the thickness of the material in units of the radiation length X_0. This is the mean distance over which a high-energy electron loses all but $1/e$ of its energy by bremsstrahlung.

(2) gives accurate results and can be used to describe multiple scattering.

2 The HERA-B detector

HERA-B [10] is an experiment originally proposed to study CP violation in the B system using an internal target at the HERA proton ring.

The HERA-B detector is a large aperture forward spectrometer (Fig. 1) with a geometrical acceptance between $0.01 < \theta < 0.22$ & $0 < \phi < 6.28$ [rads]. In GEANT [9] the detector is described by more than 30,000 volumes.

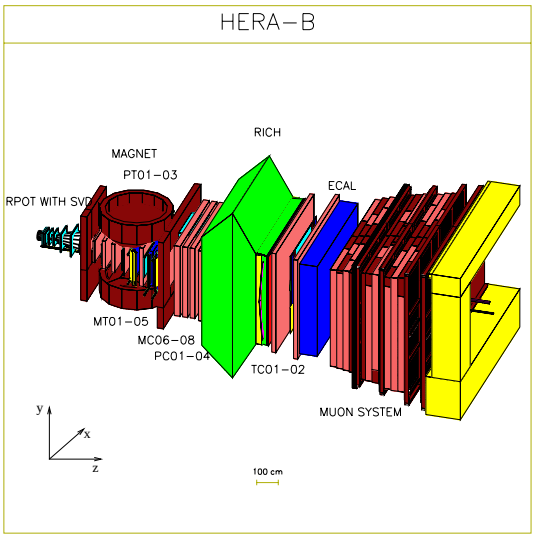

Fig. 1: *Overview of the HERA-B detector.*

In Fig. 1 one can see an overview of the HERA-B detector. The basic parts of the detector are listed below.

- **The Vertex Detector System**

  The Vertex Detector System (VDS) is defined for:

  - Primary vertex reconstruction.
  - Secondary vertex reconstruction.
  - Determination of impact parameters for tracks associated with tagging particles.

- **The Magnet**

  The HERA-B spectometer magnet is a normal-conducting dipole which provides a field integral of 2.2 mT. An integral part of the magnet system is the compensation coil which shields the electron beam so that the lepton beam may pass through HERA-B spectometer undeflected.

- **The Main Tracker**

  The particle flux which passes through the spectometer has a larger value near the beam pipe, decreasing as $\approx 1/r^2$ moving out from the beam pipe. The implications for the main tracker are that the inner region must have a segmentation which is fine enough not to be overwhelmed by the higher occupancy. As a result, the main tracker is divided into two tracking systems, the Inner Tracker and the Outer Tracker.

  The main tracker is also logically divided into three regions, labeled the TC, PC, and MC. The TC region is the area immediately downstream of the RICH, and prior to the ECAL. The PC region begins immediately downstream of the magnet and ends at the RICH and the MC region is the area inside of the magnet.

  - **The Inner Tracker** (ITR)

    The ITR consists of 10 stations of GEM MSGC (**G**as **E**lectron **M**ultiplier / **M**icro **S**trip **G**ass **C**hambers) detectors, with 184 detectors in total, each having 768 anode strips.

  - **The Outer Tracker** (OTR)

    The OTR utilizes honeycomb drift chambers as the basic unit of construction, formed from a gold/copper coated folded pokalon foil. Two different cell sizes, 5 mm and 10 mm are used, with the smaller cell size occupying the inner region of higher flux, and the 10 mm cells used in the outermost layers.

- **The RICH detector**

  The elements of the RICH detector are:

  - the C_4F_{10} gas radiator where Čerenkov photons are produced by charged particles.

– the two spherical mirrors which project Čerenkov photons to form rings on the focal surface,

– two planar mirrors which reflect the focal surface to above and below the spectometer,

– the photon detector in the focal surface

– the readout system

- **The Transition Radiation Detector** (TRD)

  The TRD is intended to complement the ECAL in the task of identifying electrons. The primary goal of this subdetector is to efficiently separate electrons from hadrons in the innermost region, where the track multiplicity is highest.

- **The Electromagnetic Calorimeter** (ECAL) The ECAL is responsible for providing the electron pretrigger signals that initiate the first level trigger algorithm.

- **The Muon Detector** The muon detector provides the muon pretrigger signals to the first level triger, as well as the information necessary for the reconstruction of muon tracks.

3 Results using only multiple scattering

In GEANT [9], one can choose which physical processes he wants to use for the simulation. We started our simulation by using only multiple scattering so to have a clear view of the difference between the results for the case we used Gaussian multiple scattering and the case we used Molière multiple scattering.

3.1 Molière multiple scattering

We will present here our results for the case the only physical process active was Molière multiple scattering. Fig. 2 is a scatter plot which shows the angular distribution (θ_{plane}) on the xz plane (the coordinate system that we use is shown in Fig. 1), versus the thickness of the material in radiation length. Here we have to say that the units we use in our simulation for the angles are [rad].

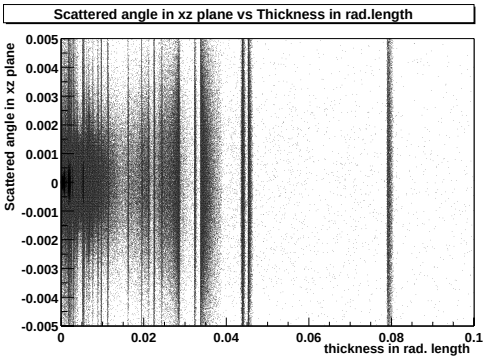

Fig. 2: *The θ_{plane} angle distribution vs thickness in rad. length.*

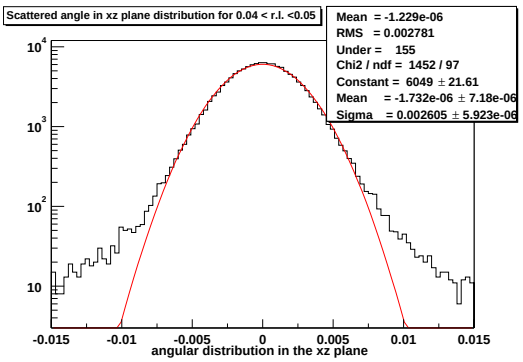

Fig. 3: *The θ_{plane} angular distribution in the x-z plane for Molière multiple scattering*

In Fig. 2 we can clearly see that geometrical volumes of the detector with specific thickness give almost all the possible angular values which corresponds to well formed lines.

Analyzing the angular distribution for a given thickness (Fig. 3) we can clearly see that it has larger tails than a Gaussian. This is the main difference between the angular distribution according to Molière and Gauss multiple scattering.

One way to study how accurate we can describe Molière multiple scattering using formula (2) is to compare the sigmas of the gaussian fit of formula (2) over some angular distributions like the one in Fig. 3, with the value obtained from formula (2). The result shown in Fig. 4 is in good agreement with the theory.

A second way to study the same thing is to take the profile histogram (the mean values) of the spatial angle distribution and compare it with the expected results of formula (2), multiplyied by $\sqrt{2}$ according to definitions of the spatial angle (Eq. (1)). We can see that the mean values plot (Fig. 5) gives bigger mean val-

ues for very thin materials than it is expected and it does not give zero.

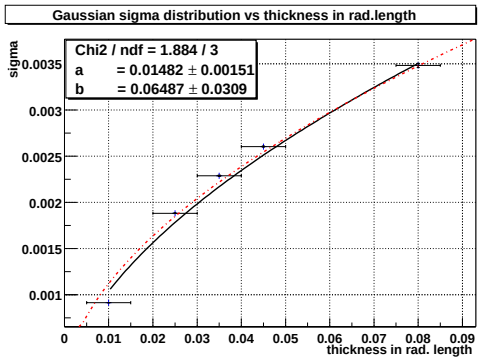

Fig. 4: *Gaussian sigmas vs thickness in rad. length. The dotted line is a plot of the formula (2), and the solid line is the fitted one.*

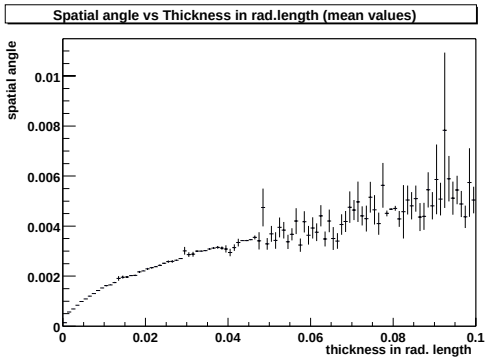

Fig. 5: *The θ^{rms}_{space} angular distribution vs thickness in rad. length.*

As a pointer to study this deviation we can use the χ^2 distribution (Fig 7) as it is given by the formula:

$$\chi^2 = \frac{(\chi_{exp} - \chi_{th})^2}{err^2} \qquad (3)$$

In formula (3), χ_{exp} is the mean angular value we obtained from the simulation (Fig 5), χ_{th} is the angular value we expect according to formula (2) and err is the error for the χ_{exp} value.

In Fig. 6, we can see that for the region of thickness, in units of radiation length, > 0.01 we have a very good agreement and almost all the deviations from the expected values are inside the error bars.

So if we exclude the region of thickness < 0.01 which gives big deviation, and make a fit over the the mean values of the angular distribution

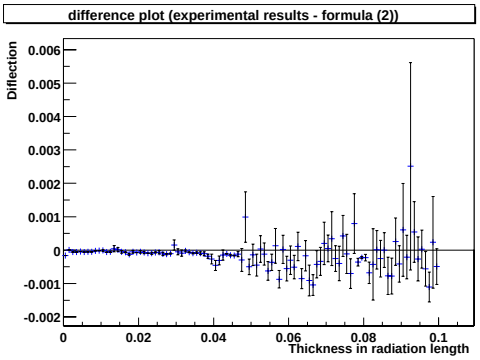

Fig. 6: *The θ^{rms}_{space} angular deviation vs thickness in radiation lengths.*

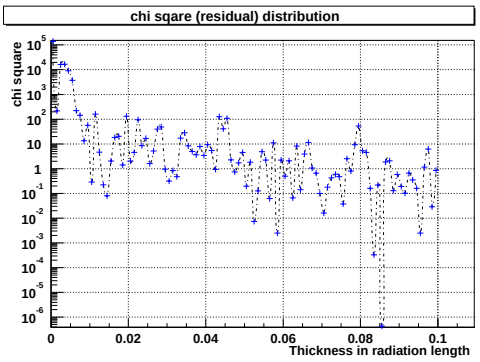

Fig. 7: *The χ^2 distribution vs thickness in radiation lengths.*

(Fig. 8), to the fotmula:

$$\theta^{rms}_{space} = \sqrt{2}\theta_0 = \alpha\sqrt{x/X_0}\,[1 + \beta ln\,(x/X_0)]\,. \qquad (4)$$

we can verify again, that there is a good agreement with the formula (2).

3.2 Gaussian multiple scattering

After we discussed the results from our simulation, using only multiple scattering according Molière theory, we will see now the results obtained using the same procedure for the case that the only physical process active in GEANT [9] is Gaussian multiple scattering.

The purpose for this analysis is to compare the results and to see the difference between the two kinds of multiple scattering.

Comparing Fig. 9 and Fig. 3 We can see the main difference between Gaussian and Molière multiple scattering, which is, as we already mentioned above, that the θ_{plane} angular distribution for Molière theory gives larger tails.

Furthermore one can see from the Figures 10

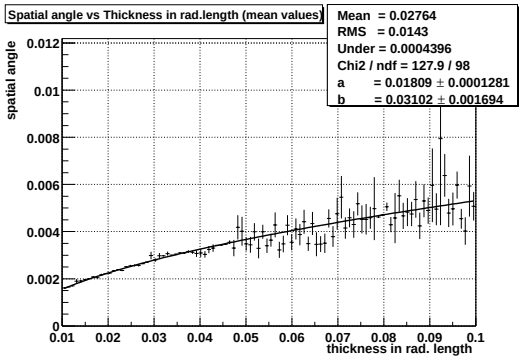

Fig. 8: *The θ^{rms}_{space} angular distribution vs thickness in rad. length and the fitted curve over this values.*

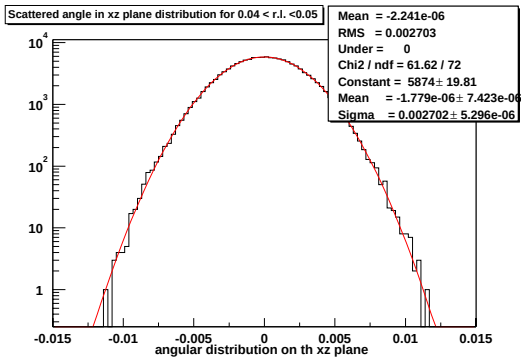

Fig. 9: *The θ_{plane} angular distribution in the x-z plane for Gaussian multiple scattering*

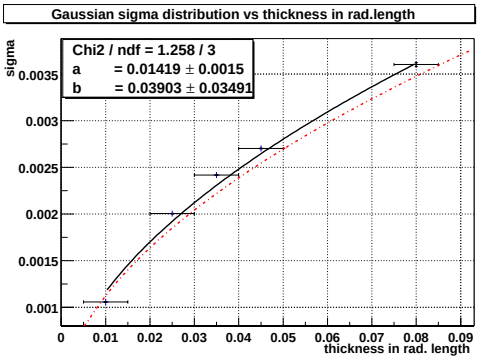

Fig. 10: *Gaussian sigmas vs thickness in rad. length. The dotted line with is a plot of the formula (2), and the solid line is the fitted one.*

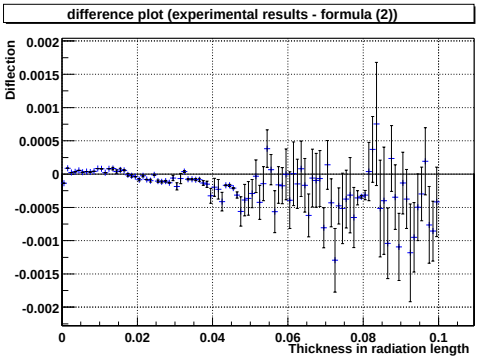

Fig. 11: *The θ^{rms}_{space} angular deviation vs thickness in radiation lengths, for Gaussian multiple scattering.*

and 13, that Gaussian multiple scattering is also well described by formula (2). But as we can see from Fig. 11 and Fig. 12 the region of thickness in radiation lengths which we have to exclude from our fit because of the deviation, is larger than the region for the case of Molière multiple scattering (now we have to exclude the region with thickness < 0.02 cm), and the deviation itself is bigger.

3.3 Results including all physical processes

In this section we show the results that we produced following the same analysis as we described above, for the case of Molière multiple scattering with all the other physical processes active. We just want to see if there are any big differences between these results and the results we discused in section *3.1*.

First of all we have to make clear what we mean when we say that all the physical processes are active, and which are these processes. We already have mentioned that in GEANT [9], one can choose which physical processes will be used for the simulation.

In our simulation the active physical processes (The default option for GEANT [9]) were the following:

- Decay in flight with generation of secondaries.
- Multiple scattering according to Molière theory.
- Continuous energy loss without generation of δ -rays and full Landau-Vavilov-Gauss fluctuations.
- Photo-electric effect with generation of the electron.
- Compton scattering with generation of e^-.
- Pair production with generation of e^-/e^+.
- Bremsstrahlung with generation of γ.
- δ -rays production with generation of e^-

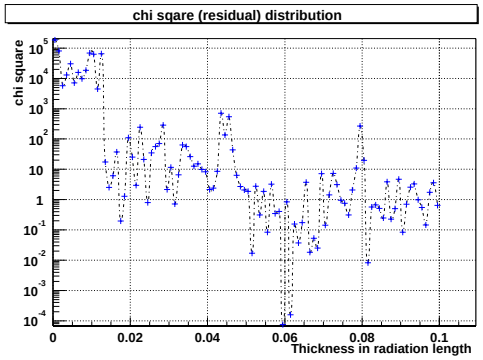

Fig. 12: *The χ^2 distribution vs thickness in radiation lengths, for Gaussian multiple scattering.*

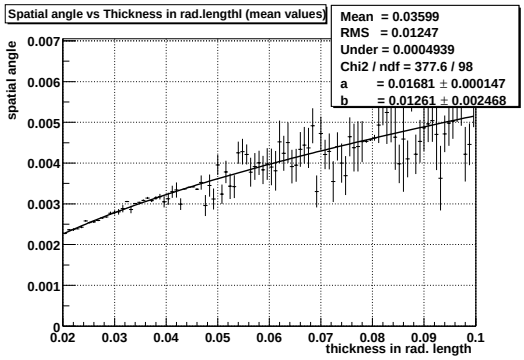

Fig. 13: *The θ^{rms}_{space} angular distribution vs thickness in rad. length and the fitted curve over this values, for Gaussian multiple scattering.*

- Positron annihilation with generation of photons.
- Hadronic interactions with generation of secondaries.
- The synchrotron radiation in magnetic field, is not simulated.

Now if we compare the results from this simulation with the results using only Molière multiple scattering we can see that they are not so different.

It has to be stated here, that in this case the deviation between the simulations results and the expected results according to formula (2) is smaller and in even more narrow region (Figs. 16, 17) But for better comparison reasons, we kept for the fitting the same cut, we used in the case of only Molière multiple scattering. The fitting results for that case are not so good, but still we can see that there is a good agreement with the theoretical predictions.

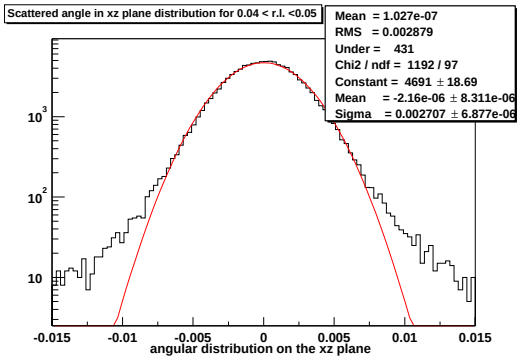

Fig. 14: *The θ_{plane} angular distribution the x-z plane, for Molière multiple scattering having all physical processes active.*

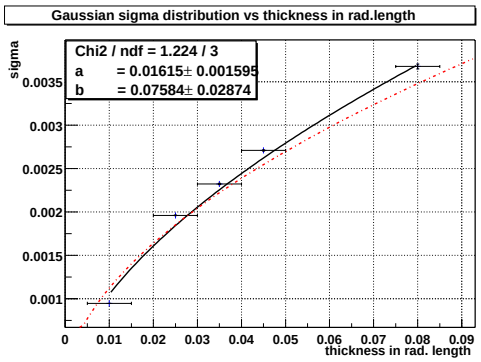

Fig. 15: *Gaussian sigmas vs thickness in rad. length, for Molière multiple scattering having all physical processes active. The dotted line is a plot of the formula (2), and the solid line is the fitted one.*

4 Conclusion

We studied the effect of multiple scattering to a 1 GeV π^- beam, traversing the HERA-B detector, using GEANT [9] Monte Carlo program. For our analysis we used three data sets obtained from the simulation. The first set gives information only for multiple scattering according to Molière theory, the second set gives information only for Gaussian multiple scattering and the third set gives information for multiple scattering according to Molière theory and for all the physical processes mentioned in subsection *3.3*.

A study of these three data sets showed that there is always a small region for very small thickness of the material, where there is a deviation between the simulated results and the theoretical expected results according to formula (2). Namely this region for Molière multiple

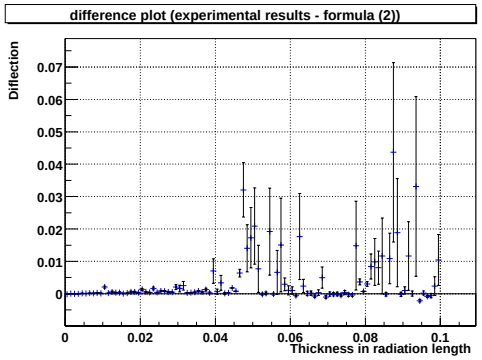

Fig. 16: *The θ^{rms}_{space} angular deviation vs thickness in radiation lengths, for Molière multiple scattering having all physical processes active.*

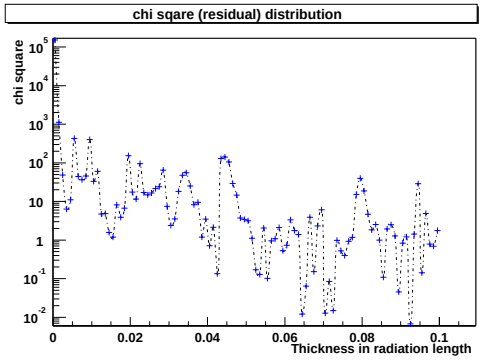

Fig. 17: *The χ^2 distribution vs thickness in radiation lengths, for Molière multiple scattering having all physical processes active.*

scattering is for thickness in radiation lengths < 0.01 cm, while for Gaussian multiple scattering the region of the deviation is for thickness in radiation lengths < 0.02 cm.

This deviation is because multiple scattering theories are not applicable for very thin materials. To overcome this limitation, single Coulomb scatterings are simulated in GEANT [9] .

So we can conclude that formula (2) describes very accurate Molière multiple scattering for material with thickness > 0.01 (in units of ratiation length) and can be used in very good agreement with the theoretical predictions.

5 Acknowledgments

I would like to thank the Zeuthen HERA-B group for making me feel welcome and for their help and support to this work. I would also like to thank my supervisor, Michael Walter and especially Siegmund Nowak for his valuable help and instructions.

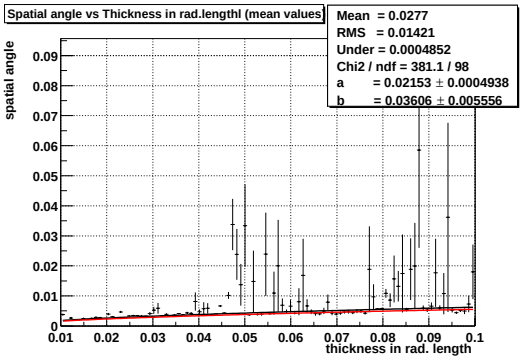

Fig. 18: *The θ^{rms}_{space} angular distribution vs thickness in rad. length and the fitted curve over this values, for Molière multiple scattering having all physical processes active.*

References

[1] G. Molière, Z. Naturforsch. **3a,** 78 (1948).

[2] H.A. Bethe, Phys. Rev. **89**, 1256 (1953).

[3] H. Snyder and W. T. Scott, Phys. Rev. **76**, 220 (1949).

[4] W.T. Scott, Rev. Mod. Phys. 35, 231 (1963).

[5] S.A. Goudsmit and J. L. Saunderson, Phys. Rev. **57**, 24 (1940).
S.A. Goudsmit and J. L. Saunderson, Phys. Rev. **58**, 36 (1940).

[6] H.W. Lewis, Phys. Rev **78**, 526 (1950).

[7] V.L. Highland, Nucl. Instrum. Methods **129**, 497 (1975).
V.L. Highland, Nucl. Instrum. Methods **161**, 171 (1979).

[8] G.R. Lynch and O.I. Dahl, Nucl. Instrum. Methods **B58**, 6 (1991).

[9] GEANT manual, CERN Program Library Long Writeup W5013.

[10] HERA-B Design Report, DESY-PRC 95/01, January 1995.